

# JCMT Legacy Release 1: 850 $\mu\text{m}$

SF Graves and the JCMT Legacy Release Team

September 2015

## 1 Overview

The JCMT is announcing the release of the JCMT Legacy Release 1 (JCMT-LR1) SCUBA-2 850  $\mu\text{m}$  data products. To aid users of JCMT products, we have produced a standardised reduction of public JCMT SCUBA-2 850  $\mu\text{m}$  observations, and made them available to download through the JCMT Science Archive (JSA) at CADC<sup>1</sup>. These reductions provide uniformly reduced coadditions of public data observed prior to 2013 August 1, and catalogues to identify the regions where emission was detected. The data have been gridded in the HEALPix HPX scheme (see Sec. 4). The calibration of the coadded tiles into  $\text{mJy arcsec}^{-2}$  is estimated to have an uncertainty of approximately 8 percent. This release was previously described in Bell et al. (2014). A more detailed description and analysis is currently being written (Graves et al 2015, in prep).

### 1.1 Key points

- Public 850  $\mu\text{m}$  SCUBA-2 observations taken between 2011-02-01 and 2013-08-01.
- Gridded onto HEALPix tiles in the HPX projection.
- All reduced using the same SMURF makemap dimmconfig 'jsa\_generic' (included in the Starlink 2015A release)
- Coadds of all the reduced non-pointing observations which passed QA coadded onto a single tile.
- Catalogues of detected ( $>5\sigma$ ) regions of contiguous emission (extents) towards each tile.
- Catalogues of local peaks within the extents of each tile.
- Over 2000 hours of observing time included.
- Search CADC with proposalID='JCMT-LR1' to view the coadds and catalogs.

---

<sup>1</sup><http://www.cadc-ccda.hia-ihp.nrc-cnrc.gc.ca/en/jcmt/>

Name	Description	Notes
Observations	Reduced individual 850 $\mu\text{m}$ observations	In units of pW & in the HPX projection.
Coadds	Coaddition of all science* observations falling on a single HPX tile	Calibrated in mJy arcsec <sup>-2</sup>
Extent Catalogues	Inventory of all contiguous regions of detected emission from within a single tile	
Peak Catalogues	List of local maxima in each extent	

\* Science observations includes standard calibration observation and PI/Survey observations, but not pointings.

Table 1: Details of the products included in the JCMT-LR1

**Please note:** Moving target observation (e.g. planets and comets) are not included in this release. Pointing observations were reduced but are not included in the coadds.

## 2 What is included in JCMT-LR1

This first release includes all publicly available 850  $\mu\text{m}$  observations observed between 2011 February 2 and 2013 August 1 towards non-moving targets. These observations have been reduced using a standardised MAKEMAP configuration developed by the JCMT for this purpose (see Sec. 3), and are gridded onto HEALPix tiles using the HPX projection (see Sec. 4). This release includes the following products: Observations, Coadds and Catalogues (see Table 1 for more details).

Users should note that all pointing observations taken during this time were reduced using this configuration and are being released; however pointings are not included in any coadds (due to their variable quality and difficulty in ensuring they were in focus in an automated fashion). Observations of moving targets (e.g. planets, comets etc.) were not included in this release.

In total, 5161 ‘science’ observations were successfully reduced onto 2930 distinct tiles, and 5519 ‘pointing’ observations were reduced individually onto 263 distinct HEALPix tiles. After excluding observations marked with a QA state of BAD (see Sec. 5), coaddition of the remaining 5059 science observations produced 2849 coadded tiles. The observed area within these tiles covers a total of 0.24 steradians (789.78 square degrees, or 1.9 per cent of the total sky).

Source detection was carried out on all of the coadded tiles, and detected emission covers  $2.91 \times 10^{-4}$  steradians (0.96 square degrees, or 0.12 per cent of the observed area).

Observations taken prior to February 2011 are not included, as these data taken in *shared risk* mode while instrument commissioning was still being conducted, and as a result

the data are more problematic to reduce and analyse (Chapin et al., 2010; Dempsey et al., 2010). Observations by the JCMT Cosmology Legacy Survey (Geach et al., 2013) are also not included as they are proprietary until 2016 March 1. Observations by PI projects form all queues, as well as the other SCUBA-2 JCMT Legacy Surveys – GBS (Ward-Thompson et al., 2007), SASSY (Thompson et al., 2007), SONS (Matthews et al., 2007), JPS (Moore et al., 2015) and NGS – were included if they fell within the given time range.

### 3 Data Reduction

SCUBA-2 observations are reduced using the Starlink SMURF programme `MAKEMAP`<sup>2</sup>. In brief, this is an iterative procedure that divides the data set into various instrumental and astronomical signals. There are an extremely large number of user-adjustable parameters that can affect the final map, depending on the science goals of the user and the details of the astronomical emission observed. For example, a cosmologist interested in detecting only faint point sources in a primarily blank map would use a distinctly different set of reduction parameters compared to a galactic astronomer looking at bright, extended and structurally complex emission from e.g. a molecular cloud. For full details on the SCUBA-2 map maker, please see Chapin et al. (2013), and the Starlink SCUBA-2 cookbook<sup>3</sup>.

#### 3.1 Configuration used in this release

The main focus in developing the *legacy* configuration used for this release was on maximising the confidence that could be placed in detection of emission, at the expense of not attempting to recover large scale structures. The JCMT-LR1 maps should not be used directly to determine the greatest extent of resolved large-scale structure. The full configuration file is located in the Starlink 2015A release, in the file `/star-2015A/share/smurf/dimmconfig_jsa_generic.lis`.

In this reduction, after the initial pre-processing stage, the SCUBA-2 mapmaker recipe uses its first few iterations to help create a mask of any unusually bright regions (`ast.skip=5` in the configuration file). This is useful since such regions may cause ringing in subsequent estimates of the low frequency noise in each bolometer. During these iterations ‘bright’ pixels are taken to be those with a signal-to-noise ratio greater than 5.0 (plus any other pixels that are attached contiguously to such pixels down the an SNR of 3 (specified by using `flt.zero_snr=5` and `flt.zero_snrlo=3`).

During all iterations an atmospheric correction is applied and data are filtered to remove any features on scales larger than 200". In addition to this a separate common-mode model is produced for each subarray (specified with `com.perarray=1`). Having a separate common mode prevents artificial flux (also known as “fake blooms”) being introduced into the map in cases where the subarray-specific common modes vary significantly and are not well represented by a single common mode. The disadvantage with having a separate common mode for each subarray is that the reduction is cannot recover emission structures on scales larger than the subarray size.

---

<sup>2</sup>see [http://www.starlink.ac.uk/cgi-bin/htxserver/sun258.htx/sun258.html?xref\\_MAKEMAP](http://www.starlink.ac.uk/cgi-bin/htxserver/sun258.htx/sun258.html?xref_MAKEMAP)

<sup>3</sup><http://starlink.ac.uk/docs/sc21.htx/sc21.html>

After the initial five iterations the recipe then performs up to 20 further iterations with all the models (specified by `numiter=-25`; the initial five iterations plus this additional 20 iterations containing all models). Each of these remaining iterations removes the astronomical signal from the residuals prior to starting the next iteration. However, to prevent instabilities in the iterative process, this subtraction only occurs within regions corresponding to bright sources. The mask identifying such sources is created in the same way as the mask used by the low-frequency noise filter (“FLT” model): source pixels are taken to be those with a signal-to-noise ratio greater than 5.0 (plus any other pixels that are attached contiguously to such pixels down to an SNR of 3 (specified by using `ast.zero_snr=5` and `ast.zero_snrlo=3`).

The map maker exits before the 20th iteration if the `maptol` parameter – the change between maps – has reached a mean value of 1% of the noise level (specified by `maptol=0.01`).

### 3.2 Effects of Masks

Recent work by S. Mairs et al. (2015, in press, MNRAS) indicates that in SCUBA-2 reductions there is a significant difference between recovery of sources inside and outside the AST mask. Sources that are outside the AST-masked regions can have their flux considerably underrepresented. The AST masked region can be thought of as roughly the region containing detectable emission in the single observation, based on the specific configuration parameters chosen. The effect is dependent on the size of the source – extended sources outside of the masked regions are poorly recovered in this reduction. To identify the regions masked in each individual observation, please look at the QUALITY mask and see the following blog post on this: <http://pipelinesandarchives.blogspot.com/2014/06/interpreting-scuba-2-map-quality-arrays.html>

## 4 HEALPix Projection and Tiling

The tiling scheme chosen for this release is that offered by HEALPix (Hierarchical Equal Area isoLatitude Pixelization, Górski et al., 2005), and is commonly used in cosmological fields. This scheme produces diamond-shaped pixels with a constant area across the whole sky; the shape however varies depending on location.

The HEALPix system starts by dividing the sky into 12 facets, and then recursively divides these cells in four at each higher resolution level. There are two standard numbering schemes used with HEALPix, of which the “nested” scheme has been used to label tiles in this release, for convenience with the HPX projection and compatibility with Virtual Observatory systems such as MOC (Multi-Order Coverage, Fernique et al., 2013).

Pixels within the individual tiles also use the HEALPix grid, which ensures that the pixelization is continuous between each tile and the adjacent tiles. This has the advantage that the tiles can be joined simply by abutting them. This is done via the HPX projection (Calabretta & Roukema, 2007) which allows the HEALPix grid to be used for conventional 2D FITS images.

While HEALPix has the advantage that all pixels have the same area, the trade off is that the pixels are not all square: they can vary in width and height while maintaining the

HEALPix parameters	
Tile Size	$\sim 1^\circ$ square
Pixels in a tile	$1024 \times 1024$
Pixel area	$3.22^2$ square arcseconds
Pixel Nside	64

Table 2: HEALPix parameters used for this release.

constant area. There are also discontinuities in the angle of the grid lines at some facet boundaries. This is largely a display problem, since while image viewers with a modern WCS implementation should be able to handle files in the HPX projection, the grid lines, and therefore astronomical sources also, bend at these positions.<sup>4</sup>

## 5 Quality Assurance

Science observations were only included in the coadds if the standard Telescope QA process had set an observation state that was not 'BAD' or 'JUNK'<sup>5</sup>.

In addition, preview images from each legacy-reduced science observation were examined by JCMT staff and marked as 'GOOD' or 'BAD'. This was primarily to avoid a) 'blooms' or 'blobs' of fake emission that can sometimes be produced at the edges of the map by the mapmaker; and b) identify the most problematic observations that had missed being flagged under the telescope standard QA process. If the observation reduction was flagged as 'BAD' at this stage it was also not included in any coadds.

Of the 5161 reduced *science* observations, 49 observations were marked as BAD and excluded from the coadditions by our manual QA process.

## 6 Calibration

The calibration of these data follows the approach used in the standard SCUBA-2 calibration paper (Dempsey et al., 2013). In brief, a Flux Conversion Factor (FCF) is derived from observations of standard calibrators of known brightnesses, which is then used to convert from the instrumental units of pW into astronomical units. For the JCMT-LR1, an average FCF was derived for the standard calibration observations taken in our time period and reduced with the legacy configuration described above. The reductions of each observation were left in the instrumental pW units, and the FCF correction was applied to the coadded tiles to produce units of mJy arcsec<sup>-2</sup>. For more information about FCFs and their derivation, please see Dempsey et al. (2013).

<sup>4</sup>If you are concerned by the visual appearance of HEALPix maps in your display and wish to reassure yourself that any apparent distortion is only due to display issues in your image viewer, we would recommend verifying the shape and position by contouring the map over a tangent plane map.

<sup>5</sup>For regular JCMT users, this standard Telescope QA process is the state of the observation as shown on the OMP webpages (<http://omp.eao.hawaii.edu>), usually set by the observer, the telescope operator or the PI of the project. 'BAD' indicates that there are serious problems with the observation, and 'JUNK' usually indicates that there is no valid astronomical signal in the observation (e.g. a closed-dome test observation).

Three commonly used SCUBA-2 calibrators have been analysed to derive an appropriate arcsecond FCF for this data set. These are Uranus, CRL 618 and CRL 2688. Note that the Uranus calibration observations are not part of the standard legacy release themselves, as observations of moving targets were not included in this release.

An arcsecond FCF was derived for the JCMT-LR1 850  $\mu\text{m}$  reduction of each calibration observation towards these three sources.<sup>6</sup> The Uranus observations from the time period covered by this release had been separately reduced using the same SCUBA-2 configuration and pixel size, but not onto a HEALPix grid due to being a moving target. The PICARD<sup>7</sup> recipe SCUBA2.CHECK\_CAL<sup>8</sup> was used to derive this arcsecond FCF.

The mean and standard deviation of the derived FCFs were calculated, using a 5-sigma clipped mean to remove extreme outliers. This removed observations with an FCF higher than 3.17 and lower than 1.78 (see Fig. 1). The final average value is:

$$\text{FCF}_{\text{arcsec},850} = 2.47 \pm 0.14 \text{ Jy pW}^{-1} \text{ arcsec}^{-2}. \quad (1)$$

The coadds in this release were calibrated using this mean FCF. This standard deviation represents a  $1\text{-}\sigma$  uncertainty of approximately 6 percent. All coadds were calibrated using the same FCF. If it is wished to undo the calibration and redo with a different value, please simply divide the data set by this FCF, and then recalibrate using the FCF of your choice. Similarly, this can be done with any flux values quoted in the catalogues derived from the coadds. A PICARD recipe (SCUBA2.UNCALIBRATE\_DATA<sup>9</sup>) is also provided as a convenience – this will set the appropriate units within the dataset.

For comparison, the usual ‘canonical’ 850  $\mu\text{m}$  arcsecond FCF used in the JCMT’s nightly reductions is  $2.34 \pm 0.08 \text{ Jy pW}^{-1} \text{ arcsec}^{-2}$  (Dempsey et al., 2013). This is approximately 5 percent lower than the value used here, and was derived using the ‘bright compact’ SCUBA-2 configuration on 1 arcsecond pixels (in comparison with the  $3.22 \times 3.22$  arcsecond pixels in this release).

To show the variation seen in the individual FCFs, we provide for reference plots of the histogram of the FCFS (Fig. 1), the variation in FCF with Tau (Fig. 2) and the variation in FCF with date (Fig. 3). No correction to the FCF for Tau or date was made in this release.

## 6.1 Uncertainty

The standard deviation of the sample of derived FCFs represents the minimum uncertainty in this calibration. In addition, we should take into account the standard error in the sub-mm flux of Uranus. Dempsey et al. (2013) quotes this as  $\pm 5$  percent. Taken together in quadrature, this gives an overall estimated error of  $\pm 8$  percent.

---

<sup>6</sup>Observations that had been marked as poor quality during QA were not included in the following analysis.

<sup>7</sup>[http://www.starlink.ac.uk/cgi-bin/htxserver/sun65.htx/sun265.html?xref\\_](http://www.starlink.ac.uk/cgi-bin/htxserver/sun65.htx/sun265.html?xref_)

<sup>8</sup>see [http://www.starlink.ac.uk/cgi-bin/htxserver/sun265.htx/sun265.html?xref\\_SCUBA2\\_CHECK\\_CAL](http://www.starlink.ac.uk/cgi-bin/htxserver/sun265.htx/sun265.html?xref_SCUBA2_CHECK_CAL)

<sup>9</sup>see [http://www.starlink.ac.uk/cgi-bin/htxserver/sun265.htx/sun265.html?xref\\_SCUBA2\\_UNCALIBRATE\\_DATA](http://www.starlink.ac.uk/cgi-bin/htxserver/sun265.htx/sun265.html?xref_SCUBA2_UNCALIBRATE_DATA)

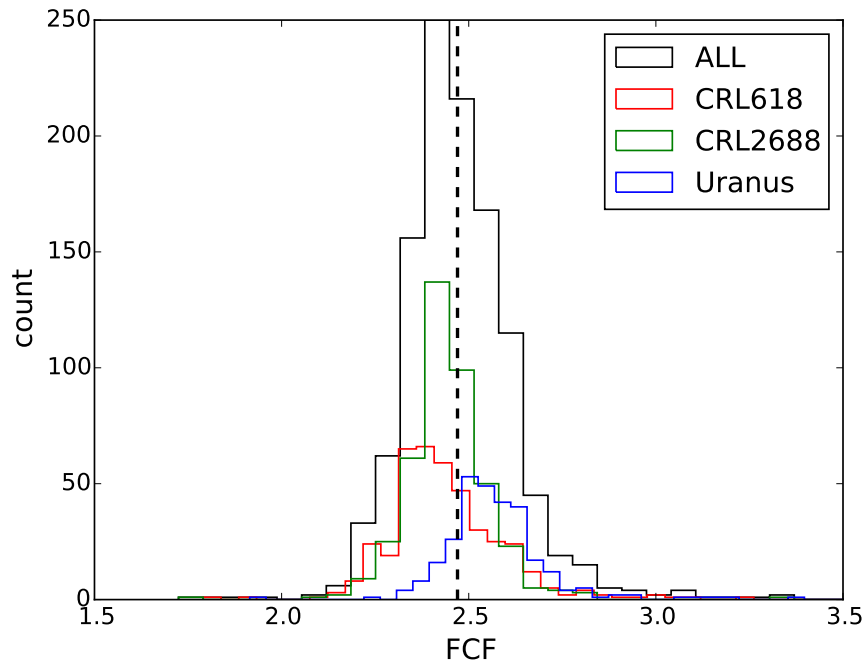


Figure 1: Histogram of FCFs, both for all sources (black) and separately for each source. The mean FCF is shown as the vertical line.

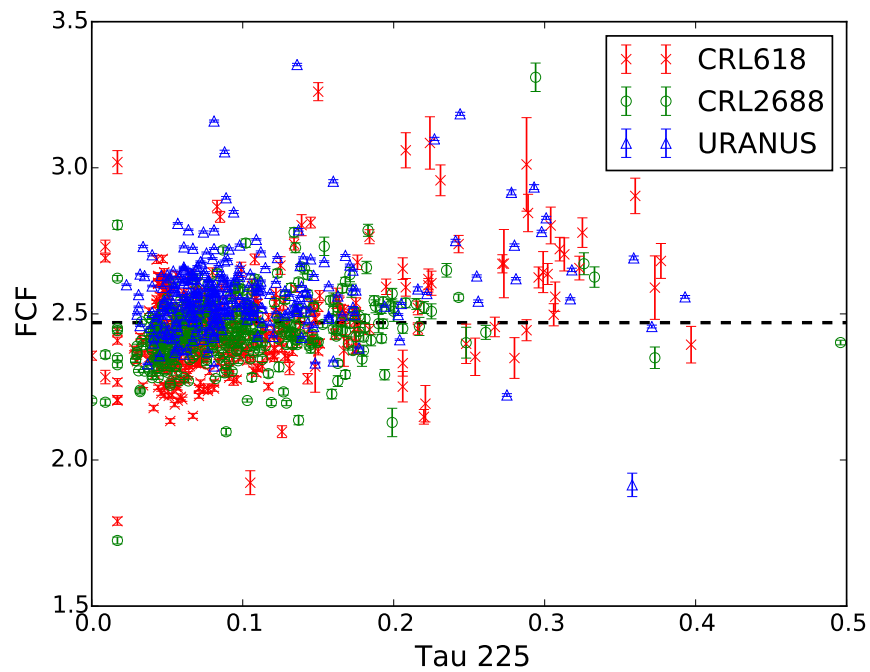


Figure 2: Derived FCF values shown against the recorded 225 GHz tau for all observations included here. The black line indicates the mean FCF.

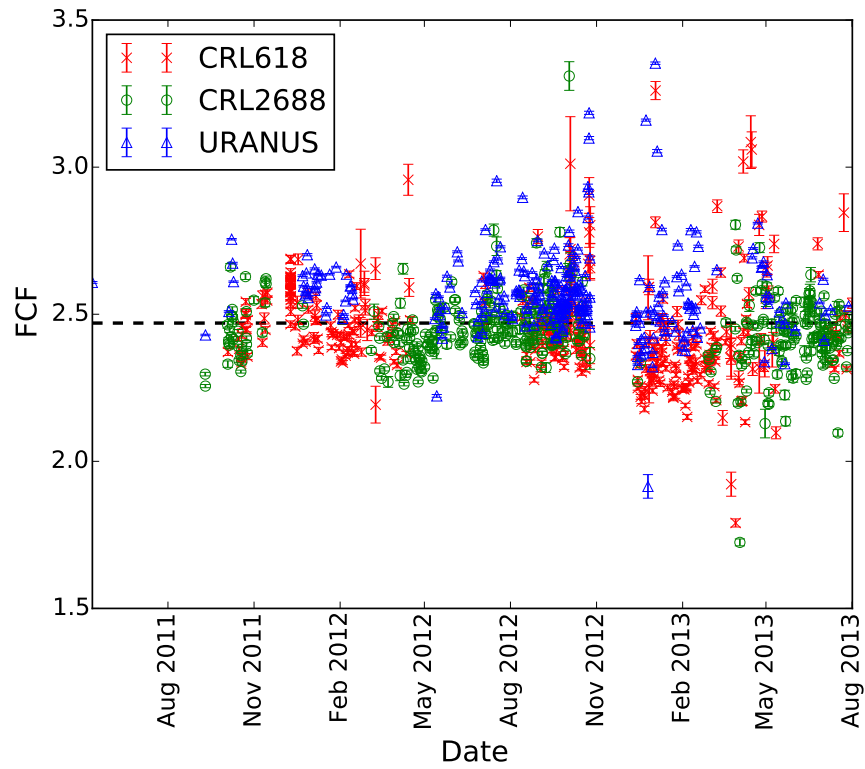


Figure 3: Derived FCF values shown against date of observation, for all observations included here. The horizontal line indicates the mean FCF.

## 7 Catalogues

The JCMT Legacy release includes emission catalogues generated from each of the coadded maps. Due to the strong large-scale filtering and the large variation in methods used to detect and characterize sources in different sections of the astronomical community, we here concentrate on two aspects of the data: a) the regions of detected emission found within the tiles (*extents*) and b) locations of local maxima within these regions of detected emission (*peaks*). The primary goal of these catalogues is to ensure it is easy for astronomers to identify regions with secure detections of emission.

We have chosen to use the Fellwalker algorithm (Berry, 2015), as implemented in the Starlink CUPID (Berry et al., 2007) package for this analysis. Unlike the more commonly used ClumpFind (Williams et al., 1994) which simply lays discrete contour levels on the map and uses those to identify regions, Fellwalker follows lines of ascent within the map to identify all peaks of emission, and has been shown to perform better when recovering information from simulations. We have found it to be robust and easy-to-understand, and to produce intelligible results.

### 7.1 Extents

We have identified the regions of contiguous extended emission within each tile by looking at the Signal-to-Noise maps of the coadded tiles. Detected regions (extents) were defined as all regions of contiguous emission containing flux brighter than  $5\text{-}\sigma$  and larger than the beam (i.e. with pixels greater than 5 in the SNR map). We followed the region down to a noise level of  $3\text{-}\sigma$ . The ‘by-eye’ QA performed on the individual maps should have removed a majority of any false emission ‘blooms’ that remained despite our chosen reduction configuration.

We used the Fellwalker algorithm as implemented in CUPID on an SNR map to produce contiguous regions of emission and to identify the position of the peak pixel within each map, and these outlines are available both as a FITS format mask file, as a HEALPix Multi-Order-Coverage file (MOC) and as a rough approximation by STC-S polygon. The catalogue for each tile indicates the ID of the clump, the RA and Dec of the peak pixel, the total flux contained within the entire extent, the flux of the peak pixel, and the area of the entire extent. We also include the approximation of the outline of the extent as an STC-S polygon string. This can be plotted with software such as GAIA or KAPPA.<sup>10</sup>

### 7.2 Peaks

In order to provide some information about the nature of emission within the extents, this release includes identification of local maxima within the extents. *It is important to note that many of these are not point sources, and that we only determine the location of peaks, not their extent.* We identified these points by running the Fellwalker algorithm (from CUPID) on the extent map. The peak detections were not derived from the SNR map but from the

---

<sup>10</sup>see <http://pipelinesandarchives.blogspot.com/2009/06/cupid-now-creates-stc-s-polygons.html>

data values. This is because by looking only within our previously identified 'extents', we have ensured that we only identified peaks towards detected emission (as opposed to noisy areas).

As our maps contain a varying noise, we used the mean noise across the entire detected extent as a representative noise. We then used the Fellwalker algorithm with that noise as the RMS value, and identified as individual local maxima those which contained a peak of  $5\text{-}\sigma$ , followed down to a noise level of  $3\text{-}\sigma$ , and with at least a  $5\text{-}\sigma$  dip between them and neighbouring maxima. Our output catalogue contains the ID of the peak, the RA and Dec of the peak pixel, the flux in the peak pixel, and the ID of the extent the peak was drawn from.

## 8 Using this dataset

For updates and more information on how to find, search and use this release please see the JCMT Science Archive page at <http://www.eaobservatory.org/jcmt/science/archive>, and the JCMT-LR1 page at <http://www.eaobservatory.org/jcmt/science/archive/lr1>.

### 8.1 Finding the Release

The JCMT LR1 dataset is available through the JCMT Science Archive (JSA, see <http://www.cadc-ccda.hia-ihp.nrc-cnrc.gc.ca/en/jcmt/>) at the Canadian Astronomy Data Centre (CADC, see <http://www.cadc-ccda.hia-ihp.nrc-cnrc.gc.ca>) and its metadata is fully integrated into the archive. JCMT-LR1 850  $\mu\text{m}$  results (observations, coadds and catalogues) will be returned as appropriate when performing normal searches within the JCMT archive, by e.g. position, time of observation or spectral coverage. The JCMT provides help and guidance for users of the JSA and CADCs advanced search interface at <http://www.eaobservatory.org/jcmt/science/archive>.

It is very easy to search for only the coadds and catalogues from this release. If you enter 'JCMT-LR1' as the **Proposal ID** on the main CADC advanced search page at <http://www.cadc-ccda.hia-ihp.nrc-cnrc.gc.ca/en/search/>, then you will have all the JCMT-LR1 coadds and catalogues returned. You can further refine your search by adding spatial constraints on the main search page, or by filtering on the results page by any of the standard columns. You can choose to see only coadds or only catalogues by selecting the appropriate **Data Type** (image or catalogue) from the **Additional Constraints** section of the main search page.

When looking at the results page, preview images on the results page are available to show you an image of the whole tile, or an image of the detected extents or peaks as appropriate for the product type in question. Please note that when even if no emission is detected, there will still be an entry for **extent-cat** in the search results. This is so the auxiliary MOC file (see Sec. 8.5) giving the footprint of the tile can be downloaded. The preview image will say 'No emission detected' to make this clear.

	File Name	productID	algorithm
<b>Single obs.</b>	jcmts<YYYYMMDD>_<XXXXXX>_850 _healpix<ZZZZZZ>_obs_000.fits	healpix-850um	exposure
<b>Coadd</b>	jcmts850um_healpix<ZZZZZZ> _pub_000.fits	healpix-850um	public
<b>Extent Cat.</b>	jcmts850um_extent-cat<ZZZZZZ> _pub_000.fits	extent-850um	public
<b>Peak Cat.</b>	jcmts850um_peak-cat<ZZZZZZ> _pub_000.fits	peak-850um	public

<YYYYMMDD> is the UT date of the observation  
 <XXXXXX> is the scan number of the observation  
 <ZZZZZZ> is the HEALPix tile number

Table 3: The naming schemes used for the filenames, productIDs and algorithms, as shown at CADC.

## 8.2 File name convention

When downloading observations, coadds and catalogues, please note that we have used naming scheme given in Table 3 for our products. The **productID** is a piece of CADC metadata that helps you identify what a given row in your results is. The **algorithm** represents how the observations that went into a given data product were chosen. You can filter by the productID and the algorithm when looking at the results of a CADC search.

## 8.3 Using HPX gridded HEALPix tiles

Much of the JCMT supported Starlink software should handle using HPX gridded HEALPix tiles directly and without conversion. They can be opened in GAIA directly and viewed and/or analysed there. They can also be contoured over maps in other projections within GAIA. To download and setup the Starlink software, please follow the instructions at <http://starlink.eao.hawaii.edu>.

However, as mentioned earlier image-viewers will usually display the pixels as square, regardless of their true shape, causing an apparent distortion to the viewer. In addition, many users will prefer to deal with their data in a more standard tangent plane projection.

To reproject a set of JSA tiles into a tangent plane projection with square pixels and with celestial north pointing upwards, the SMURF command `jsajoin` can be used. Please see [http://www.starlink.ac.uk/cgi-bin/htxserver/sun258.htx/sun258.html?xref\\_JSAJOIN](http://www.starlink.ac.uk/cgi-bin/htxserver/sun258.htx/sun258.html?xref_JSAJOIN) for full directions on how to use this command.

If you are happy using the files in their native HPX projection, then you can join multiple tiles together simply by abutting them using the KAPPA paste command - see [http://www.starlink.ac.uk/cgi-bin/htxserver/sun95.htx/sun95.html?xref\\_PASTE](http://www.starlink.ac.uk/cgi-bin/htxserver/sun95.htx/sun95.html?xref_PASTE).

The standard Starlink 'KAPPA' command `wcsalign` can of course still be used to align an HPX file with a map in almost any other projection - see [http://www.starlink.ac.uk/cgi-bin/htxserver/sun95.htx/sun95.html?xref\\_WCSALIGN](http://www.starlink.ac.uk/cgi-bin/htxserver/sun95.htx/sun95.html?xref_WCSALIGN) for full details.

Please note that CADC provide our files in the standard FITS format. To convert to the Starlink NDF format (Jenness et al., 2014) used by KAPPA and SMURF commands, you can use the Starlink command `fits2ndf`, or by loading the package CONVERT in a terminal subsequent Starlink commands will automatically perform on-the-fly conversion of FITS files.

## 8.4 Catalogues

We have provided our extent and peak catalogues in the standard FITS format. These can be opened in GAIA as a local catalogue, and viewed aligned over the top of any displayed image. TOPCAT, shipped with Starlink, also provides an extremely sophisticated means of viewing and interacting with catalogues.

In the catalogues, the identifier for each extent or peak uses a standardised form based on the position of the peak pixel. This follows:

- **Extents:** JCMTPX\_J<HHMMSS.S><±DDMMSS>
- **Peaks:** JCMTPP\_J<HHMMSS.S><±DDMMSS>

Where HHMMSS.S is the sexagesimal Right Ascension, and DDMMSS is the sexagesimal Declination.

## 8.5 MOC files

As a convenience, we have provided HEALPix based Multi-Order-Coverage files (see <http://ivoa.net/documents/MOC/> representing the footprint of our observations and regions of detected emission. These are downloaded along with the extent catalogues as an auxiliary file. These files are not currently supported by Starlink software, but are viewable in Aladin (<http://aladin.u-strasbg.fr/>).

## References

- Bell G. S., et al., 2014, in Chiozzi G., Radziwill N. M., eds, Proc. SPIE Vol. 9152, Software and Cyberinfrastructure for Astronomy III. p. 2, doi:10.1117/12.2054983
- Berry D. S., 2015, Astronomy and Computing, 10, 22
- Berry D. S., Reinhold K., Jenness T., Economou F., 2007, in Shaw R. A., Hill F., Bell D. J., eds, ASP Conf. Ser. Vol. 376, Astronomical Data Analysis Software and Systems XVI. p. 425
- Calabretta M. R., Roukema B. F., 2007, MNRAS, 381, 865
- Chapin E., Dempsey J., Jenness T., Scott D., Thomas H., Tilanus R., 2010, Starlink Cookbook 19, The SCUBA-2 SRO Data Reduction Cookbook, <http://www.starlink.ac.uk/docs/sc19.htx/sc19.html>. Joint Astronomy Centre, <http://www.starlink.ac.uk/docs/sc19.htx/sc19.html>

Chapin E. L., Berry D. S., Gibb A. G., Jenness T., Scott D., Tilanus R. P. J., Economou F., Holland W. S., 2013, MNRAS, 430, 2545

Dempsey J. T., Friberg P., Jenness T., Bintley D., Holland W. S., 2010, in Holland W. S., Zmuidzinas J., eds, Proc. SPIE Vol. 7741, Millimeter, Submillimeter, and Far-Infrared Detectors and Instrumentation for Astronomy V. p. 77411X (arXiv:1008.0890), doi:10.1117/12.856476

Dempsey J. T., et al., 2013, MNRAS, 430, 2534

Fernique P., Durand D., Boch T., Oberto A., Pineau F., 2013, in Friedel D. N., ed., Astronomical Society of the Pacific Conference Series Vol. 475, Astronomical Data Analysis Software and Systems XXII. p. 135

Geach J. E., et al., 2013, MNRAS, 432, 53

Górski K. M., Hivon E., Banday A. J., Wandelt B. D., Hansen F. K., Reinecke M., Bartelmann M., 2005, ApJ, 622, 759

Jenness T., et al., 2014, preprint, (arXiv:1410.7513)

Matthews B. C., et al., 2007, PASP, 119, 842

Moore T. J. T., et al., 2015, preprint, (arXiv:1509.00318)

Thompson M. A., et al., 2007, preprint, (arXiv:0704.3202)

Ward-Thompson D., et al., 2007, PASP, 119, 855

Williams J. P., de Geus E. J., Blitz L., 1994, ApJ, 428, 693